national accelerator laboratory

TM-233
2123

DESIGN CRITERIA FOR A HIGH ENERGY, HIGH RESOLUTION FOCUSING SPECTROMETER

K. P. Pretzl

April 1970

I. INTRODUCTION

A high energy, high resolution focusing spectrometer is, no doubt, a very powerful instrument for measuring two-body elastic and inelastic reactions in the multi-GeV region. The design of such a system is concerned with matching the experimental desirability with the technical feasibility; the former has no natural boundary but the latter has.

The aim of this report is to evaluate design criteria for high energy focusing spectrometers in general, and to compare the results with non-focusing systems of the same quality.

II. MOMENTUM RESOLUTION AND SOLID ANGLE ACCEPTANCE

From the many parameters, which influence the design of a spectrometer, the experimentalist is mainly concerned with two; the momentum resolution $\frac{\Delta p}{p}$ and the solid angle acceptance $\Delta\Omega$ of the system. The momentum resolution of a spectrometer determines the accuracy, with which the momentum transfer or the missing mass for a particular reaction can be measured, provided the incident momentum of the particles is well known. The angular acceptance determines the angular range, within

which the differential cross-section of a reaction can be measured, and is directly proportional to the event rate for a given reaction cross-section, a given incident particle flux, and a given target density.

The momentum resolution of any point-to-point imaging system is given by a very general formula[1]

$$\frac{\Delta p}{p} = \frac{4(x_o \theta_o) B\rho}{\phi} \qquad (1)$$

$B\rho$ is the magnetic rigidity in kGm and is equal to $B\rho = 33{,}356\ p$, where p is the particle momentum in GeV/c. The phase space $4(x_o \theta_o)$ in the bending plane, which is determined by the spot size $2x_o$ of the incident particle beam at the experimental target and the angle $2\theta_o$, is in the following calculations for simplicity reasons assumed to be rectangular as indicated in Fig. 1. The magnetic flux ϕ is the product of the field B in the bending magnet and the Area A, which is enclosed by the extreme rays through the magnet as schematically shown in Fig. 2.

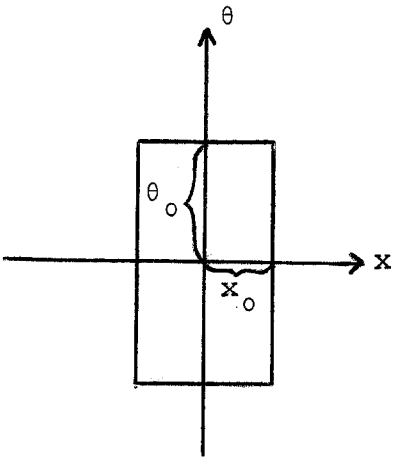

Fig. 1

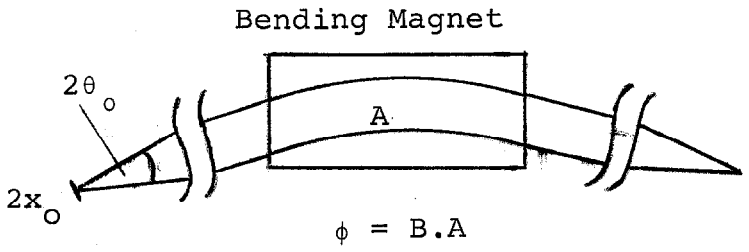

Fig. 2.

In order to achieve high resolution with focusing spectrometers the following general conclusion can be drawn from formula (1):

1. The spot-size $2x_o$ has to be kept as small as possible. This point will be evaluated in more detail later in this report.
2. The magnetic flux ϕ should be as large as possible. It should be kept in mind that ϕ and θ_o, therefore the solid angle acceptance $\Delta\Omega$ of the system, are not independent of one another.

Figure 3 illustrates very schematically a focusing spectrometer, which has been used as an example for the following studies:

The particles coming from an experimental Target T will be point-to-parallel focused horizontally and vertically by a quadrupole doublet Q_1 (vertically focusing), Q_2 (horizontally focusing). They travel parallel to the optical axis of the system through several bending magnets BM_1, BM_2, BM_3 until they are focused by a parallel-to-point doublet Q_3 (horizontally focusing), Q_4 (vertically focusing) into an image plane I. The quadrupole doublet 1 (Q_1Q_2) and doublet 2 (Q_3Q_4) are symmetric, therefore are the angular and the linear magnification in both planes 1:1. The quadrupoles Q_1, Q_2, Q_3 and Q_4 are of the same physical size with a length L and a bore 2R. The distance D between the quadrupoles in each doublet has been kept as small as possible in order to achieve a maximum solid angle acceptance of the system.

High Energy High Resolution Spectrometer

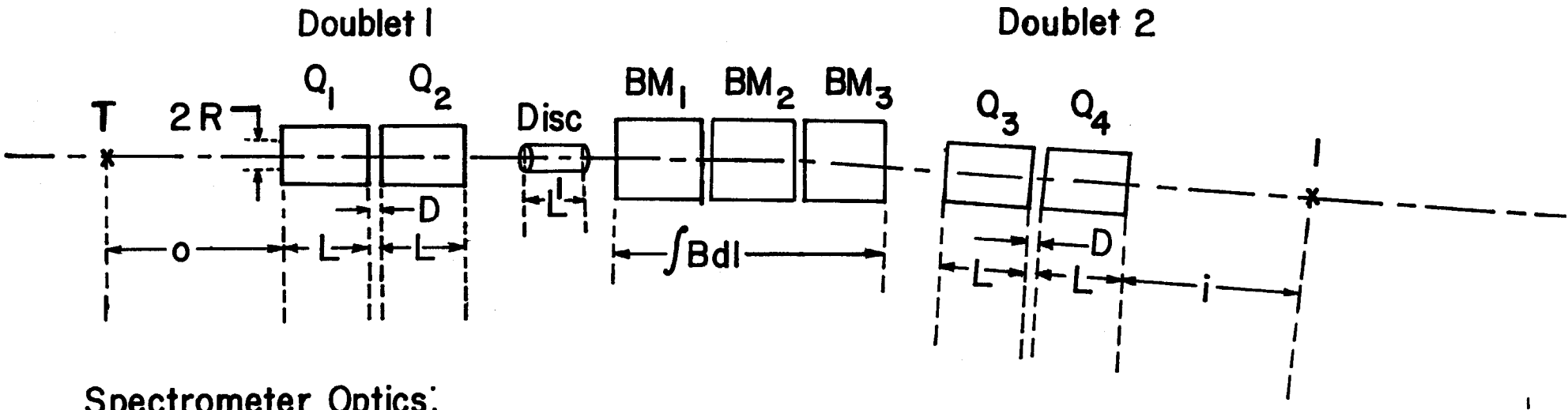

Spectrometer Optics:

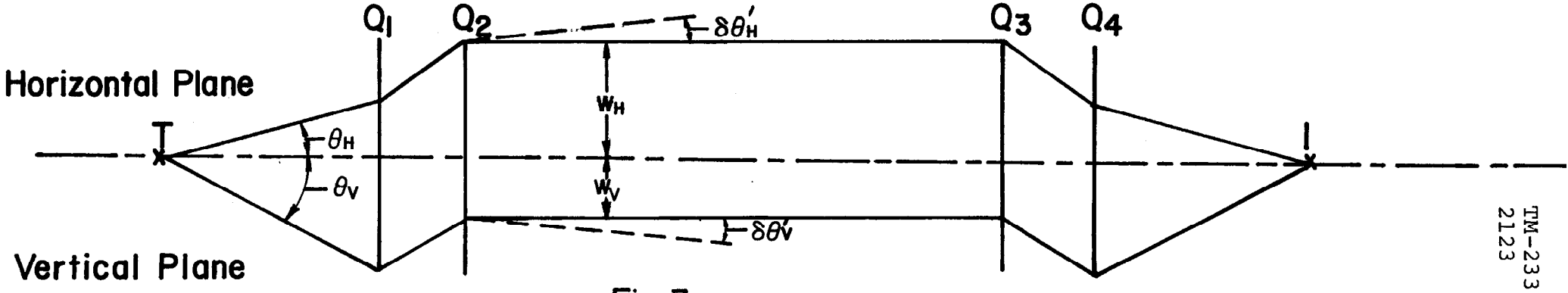

Fig. 3

TM-233
2123

This particular choice of beam optics for a high energy resolution spectrometer has the following advantages.

1. The distance between the two quadrupole doublets does not affect the solid angle acceptance of the system for particles within a certain momentum bite, nor does it affect the momentum resolution of the system. The over-all length of the spectrometer is only determined by the length L of the quadrupoles, the length of the bending magnets and the longitudinal dimensions of detectors (Čerenkov-counters), which might be placed in between the quadrupole doublets 1 and 2 (Fig. 3). This feature is very desirable if housing and mounting costs are considered for such a system.

2. A DISC Čerenkov counter can be placed in the parallel section of the beam (Fig. 3). Effects of chromatic aberrations in Q_1 and Q_2 on the resolution of the DISC counter are evaluated in Chapter IV.

3. Second order corrections due to fringe field effects and pole-tip rotations in the bending magnets are minimized in both planes (horizontally and vertically).

4. A focusing spectrometer makes maximum use out of the bending magnets and is most economically designed, if the width W of the constant field region of the bending magnets is covered by the extreme rays, i.e.,

if the beam is going parallel with the width W through the bending plane. From Fig. 3 and formula (1) it is apparent to momentum analyze the particles in the horizontal plane, where the initial phase space is smallest and the area A defined by the extreme rays through the bending magnets is largest, whereas the vertical plane, with the larger angular acceptance $2\theta_V$, determines the angular range within which the cross-section of a particular reaction can be measured.

For 200 GeV particles, the maximum angular acceptance θ_H, θ_V and solid angle acceptance $\Delta\Omega$ of a point-to-parallel doublet with a distance D = 30cm, has been studied versus the quadrupole length L, which was kept equal for both quadrupoles. A conservative value for the maximum pole tip field B_{max}= 10kG and a bore of 2R = 10cm (=4") was chosen, which yield a maximum gradient ∇B_{max}= 2kG/cm = 5kG/inch. In order to keep the focal lengths F_x (horizontal) and F_y (vertical) of the doublet as short as possible, one of the quadrupoles was always assumed to operate with maximum gradient. However, the ratio of the gradients varied from $\frac{\nabla B_{Q2}}{\nabla B_{Q1}} \approx 1$ (for L = 2m) to $\frac{\nabla B_{Q2}}{\nabla B_{Q1}} \approx 0.5$ (for L = 8m).

Figure 4 illustrates the results which have been obtained from W. Baker's Tables "Properties of Quadrupole Magnet Doublets" (BNL-795). The momentum resolution $\frac{\Delta p}{p}_H$ (horizontal bending) and $\frac{\Delta p}{p}_V$ (vertical bending) for a given $\int Bd\ell$ = 250kGm, a given spot size $2x_o$ = 1mm and a given

magnification 1:1 has been calculated from formula (1) and is also shown in Fig. 4. The momentum acceptance of the spectrometer is ±5%. It is normally not so much limited by the magnet apertures, but by the longitudinal displacement of the focal point.

The experimentalist is usually interested in the momentum transfer region covered by the angular acceptance of the spectrometer. The transverse momentum square, which can be approximated at small scattering angles θ_{lab} to $t = -p^2\theta_{lab}^2 [GeV/c]^2$, has been calculated and plotted versus the vertical angular acceptance θ_V of the spectrometer for an incident particle momentum p = 200 GeV/c (Fig. 5). By either turning the spectrometer around its pivot, or by changing the angle of the beam hitting the target, the angular range can be enlarged.

As an example, the momentum resolution

$$\frac{\Delta p}{p} = \frac{2x_o 2\theta_H B\rho}{2W_H \int Bd\ell} \qquad (2)$$

versus $\int Bd\ell$ has been evaluated for the following initial parameters:

$$L = 6m \qquad (3a)$$
$$o = i = 12m$$

$$2x_o = 1mm \text{ spot size} \qquad (3b)$$

$$\left.\begin{aligned} 2\theta_H &= 2.66 \text{ [mrad]} \\ 2\theta_V &= 7.5 \text{ [mrad]} \end{aligned}\right\} \text{ (see also Fig. 3)} \qquad (4)$$

$$W_H = F_H \theta_H \approx 5(cm) \qquad (5)$$

$$B\rho = 33.356\ p = 6.7\ 10^3 \text{ [kGm]} \qquad (6)$$

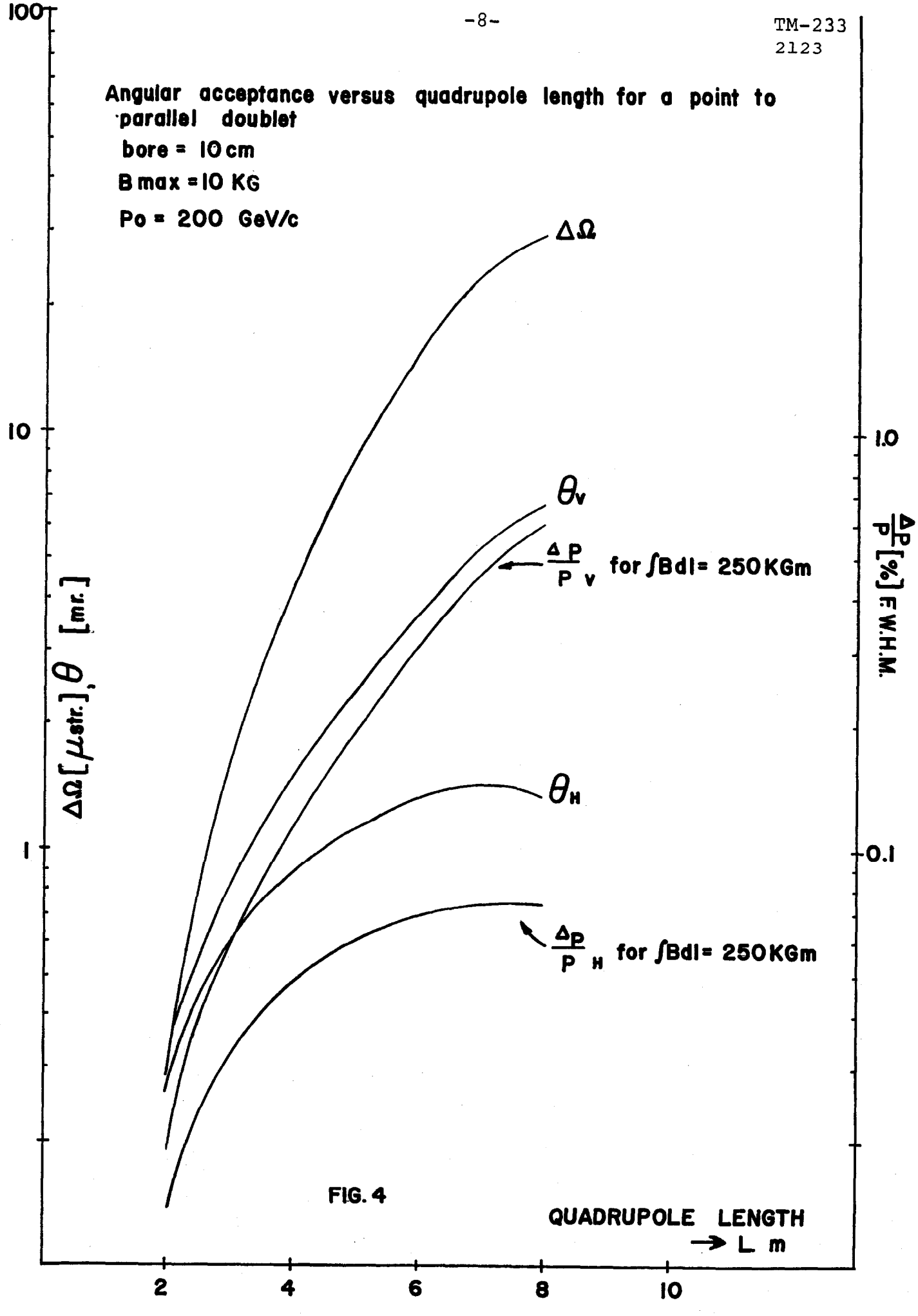
Angular acceptance versus quadrupole length for a point to parallel doublet
bore = 10 cm
B max = 10 KG
Po = 200 GeV/c
ΔΩ
θv
Δp/p v for ∫Bdl = 250 KGm
θH
Δp/p H for ∫Bdl = 250 KGm
100
10
1
1.0
0.1
ΔΩ [μstr.], θ [mr.]
Δp/p [%] F.W.H.M.
QUADRUPOLE LENGTH → L m
2
4
6
8
10

FIG. 4

Transverse Momentum Squared t Versus Angular Acceptance θ_v at 200GeV/c

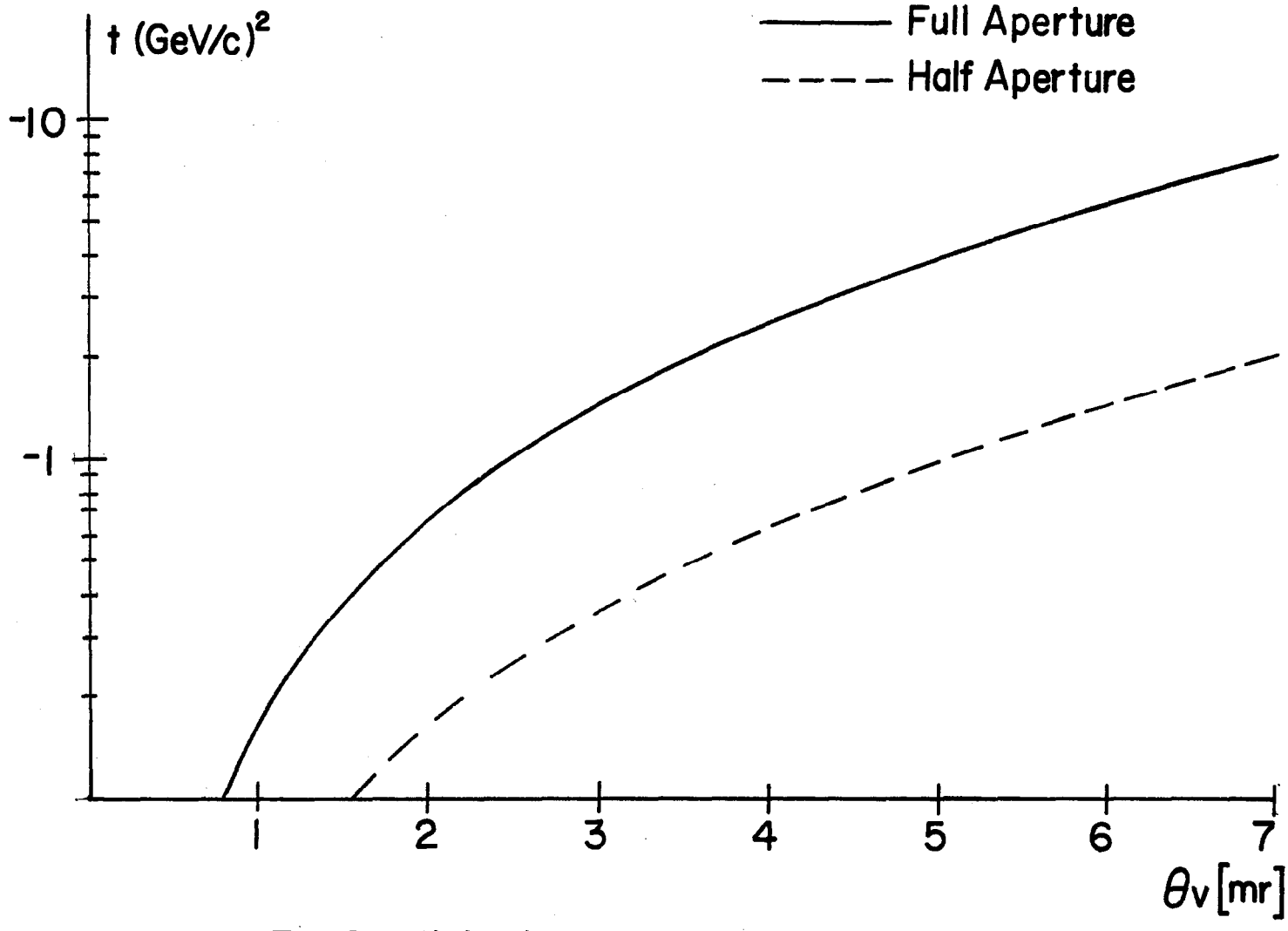

For Small Angle

$$t \approx -p^2 \theta^2_{LAB} \ [GeV/c]$$

Fig.5

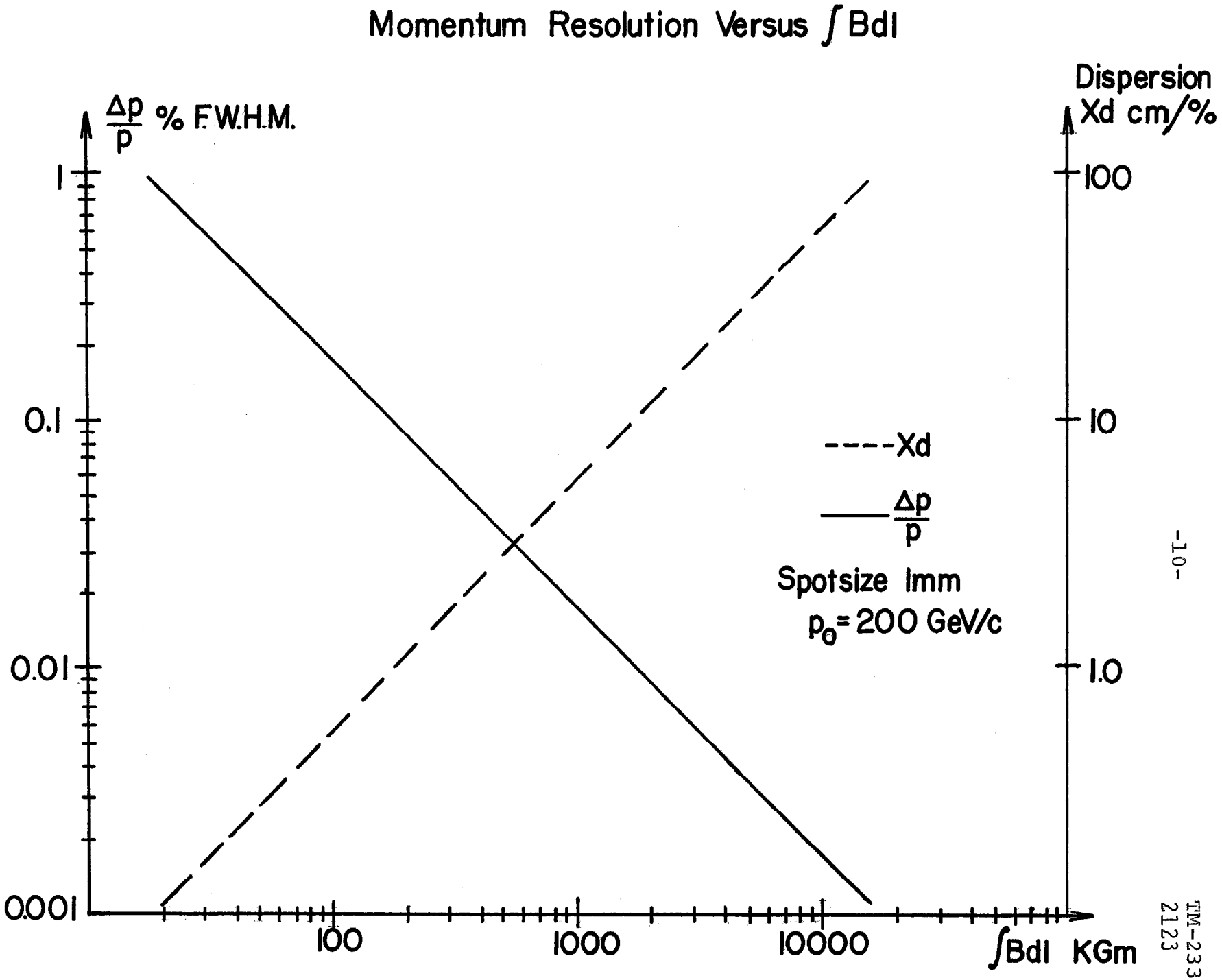

Fig.6

TM-233
2123

Assuming a 1:1 magnification, the dispersion x_d is given then by

$$x_d = \frac{2x_o}{\frac{\Delta p}{p}} \text{ [mm/\%]} \qquad (7)$$

The results are shown in Fig. 6. In this calculation we assumed a perfect field homogenity within the width $2W_H$ and the effective length of the bending magnets.

III. IMPROVEMENTS ON $\frac{\Delta p}{p}$ AND THEIR LIMITS

By chopping off the phase space, i.e., by measuring positions in the object plane, the momentum resolution of a spectrometer can usually be improved. This can be done in many ways by introducing different kinds of detectors (scintillation counter hodoscopes, wire planes, proportional wire planes....) at different places in the system. In any case, the improvement of $\frac{\Delta p}{p}$ is limited entirely by the spatial resolution of the particular detector. The nice feature about it is, that by measuring the position in the object and image plane, the momentum resolution of the spectrometer for a given $\int B d\ell$ is no more dependent on the beam spot size, but on the accuracy of the position measurement. However, the particle flux one can possibly handle with the spectrometer is determined by the deadtime of the detectors.

In order to evaluate this effect more quantitatively we have introduced as an example three proportional wire chambers W_1, W_2, W_3 in our system as shown in Fig. 7.

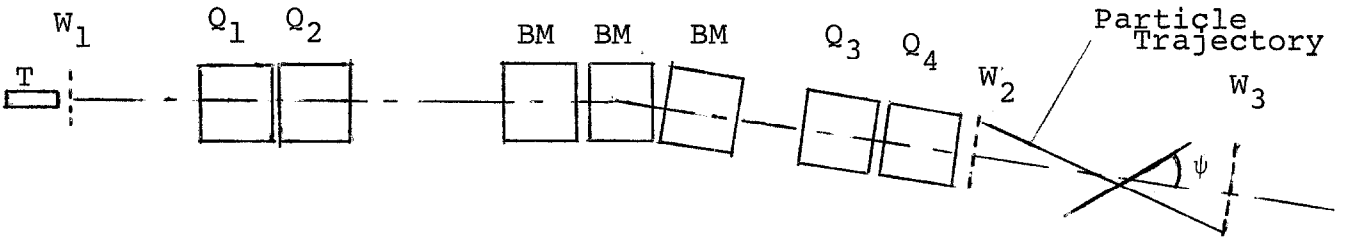

ψ = focal plane tilt due to chromatic aberration

Fig. 7

Each chamber was assumed to be made out of two wire planes x and y with a 2mm wire spacing in each plane, which yield a spatial resolution of approximately $\Delta x = \Delta y = \pm 0.5$mm in each plane.

Since a particle with the momentum p, with a horizontal displacement x_1 and an angle x_1' at the object plane W_1 will have the coordinate

$$x_3 = R_{11}x_1 + R_{12}\,x_1' + R_{16}\,\frac{\Delta p}{p} \qquad (8)$$

in plane W_3 and since R_{12} vanishes at $p = p_o$ or is very small, in the neighborhood of p_o, only the horizontal components of the chambers W_1 and W_3 are sufficient to determine the Δp of the particle in first order. R_{11}, R_{12}, R_{16} are the matrix elements of the transfer matrix R. The maximum resolution can be obtained if W_1 and W_3 are placed right at the foci. This is one of the principal advantages of a focusing over a

non-focusing spectrometer.

Because of chromatic aberration in the quadrupoles, and because of second order effects in the bending magnets, due to fringe field effects and pole-tip rotation, in the case of non-wedge shaped bending magnets, the image plane is tilted by an angle ψ (Fig. 7). The angle ψ is generally very small, on the order of a few degrees and smaller. The tilt of the image plane can be calculated in second order by the program "Transport"[2], and in higher order by appropriate ray tracing programs (Enge, Kowalski). The smear of the spot-size δx_3 per percent $\frac{\Delta p}{p}$ due to this second order effect is proportional

$$\delta x_3 \approx \frac{\theta x}{\psi} x_d \qquad (9)$$

where θx is the horizontal beam divergence at the image. It is clear from formula (8) that δx_3 can be reduced to a minimum by measuring the angle of the particle trajectory with chambers W_2 and W_3. The final spot-size in the horizontal image plane is then approximately given by

$$\Delta x_3 = R_{11} \Delta x_1 + \delta x_3 \qquad (10)$$

By introducing W_2 one is also able to measure in first or higher order, the scattering angle

$$x_1' = R_{21}' x_3 + R_{22}' x_3' + R_{26}' \frac{\Delta p}{p} + \text{higher order terms} \qquad (11)$$

at the target, where R_{21}', R_{22}' and R_{26}' are now the matrix elements for the inverse transfer matrix R'. The same statement applies for the y plane, since W_1 W_2 W_3 measure coordinates

in both the x and y planes. The accuracy in determining x_1' or y_1' is given by the product

$$\Delta x_1' = \Delta x \sqrt{\frac{2}{d}} R_{22}'$$
$$\Delta y_1' = \Delta y \sqrt{\frac{2}{d}} R_{44}' \qquad (12)$$

where d is the distance between the chambers W_2 and W_3. We have chosen d = 12m, which corresponds approximately to the image distance of our spectrometer. Figure 8 shows the momentum resolution $\frac{\Delta p}{p}$, which is now independent of the beam spot-size, versus $\int Bd\ell$ obtained with this set of proportional wire chambers W_1 W_2 W_3. The calculation has been based on the parameters (3a) (4) (5) (6), a 1:1 magnification and on the assumption of a negligibly small δx_3. Also shown in Fig. 8 is the momentum resolution $\frac{\Delta p}{p}\Big|_{lim}$ versus $\int Bd\ell$ limited by the multiple scattering in the wire planes. A general method for calculating multiple scattering effects in any focusing system is described in the appendix of this report, therefore, it will not be discussed here in detail. The multiple scattering in the chamber W_1 and W_3 can be neglected, since W_1 represents the object plane and W_3 is the last chamber.

The multiple scattering in the proportional chamber W_2 and its effect on the spot-size Δx_3 in the horizontal image plane has been calculated for p = 200 GeV/c

$$\Delta x_3 = \Delta \alpha_2 \quad d = \pm 0.041 [mm] \qquad (13)$$

with a multiple scattering angle

$$\Delta\alpha_2 = \frac{15(\text{MeV})}{p.v(\text{MeV})}\sqrt{\frac{L}{L_o}} = \pm 3.4\ 10^{-6}\ [\text{rad}] \qquad (14)$$

and with $\frac{L}{L_o} = 2.10^{-3}$, which we obtained for 100μ Cu wires with a density effect of $\frac{1}{12}$, for 100μ mylar windows and for a 1.5cm particle path length through neon gas. The momentum resolution limited by the multiple scattering is then given by

$$\frac{\Delta p}{p}\Big|_{lim} = \frac{\Delta x_3}{xd} \qquad (15)$$

We draw the following very important conclusions:

1. For a given $\int Bd\ell$, the momentum resolution of a focusing spectrometer can be drastically improved and can be made independent of the beam spot-size, if detectors like W_1 W_2 W_3 with a high spatial resolution are introduced. Or in other words, for a given $\frac{\Delta p}{p}$ one is able to save money on a usually very costly $\int Bd\ell$ with a good spatial resolution in the detectors W_1 W_2 W_3.

2. At 200 GeV/c the spatial resolution in the detectors W_1 W_2 W_3 can be improved by one order of magnitude before $\frac{\Delta p}{p}$ reaches its multiple scattering limit. This statement applies also for similar detectors and their present spatial resolution like scintillation counter hodoscopes and ordinary wire spark chambers.

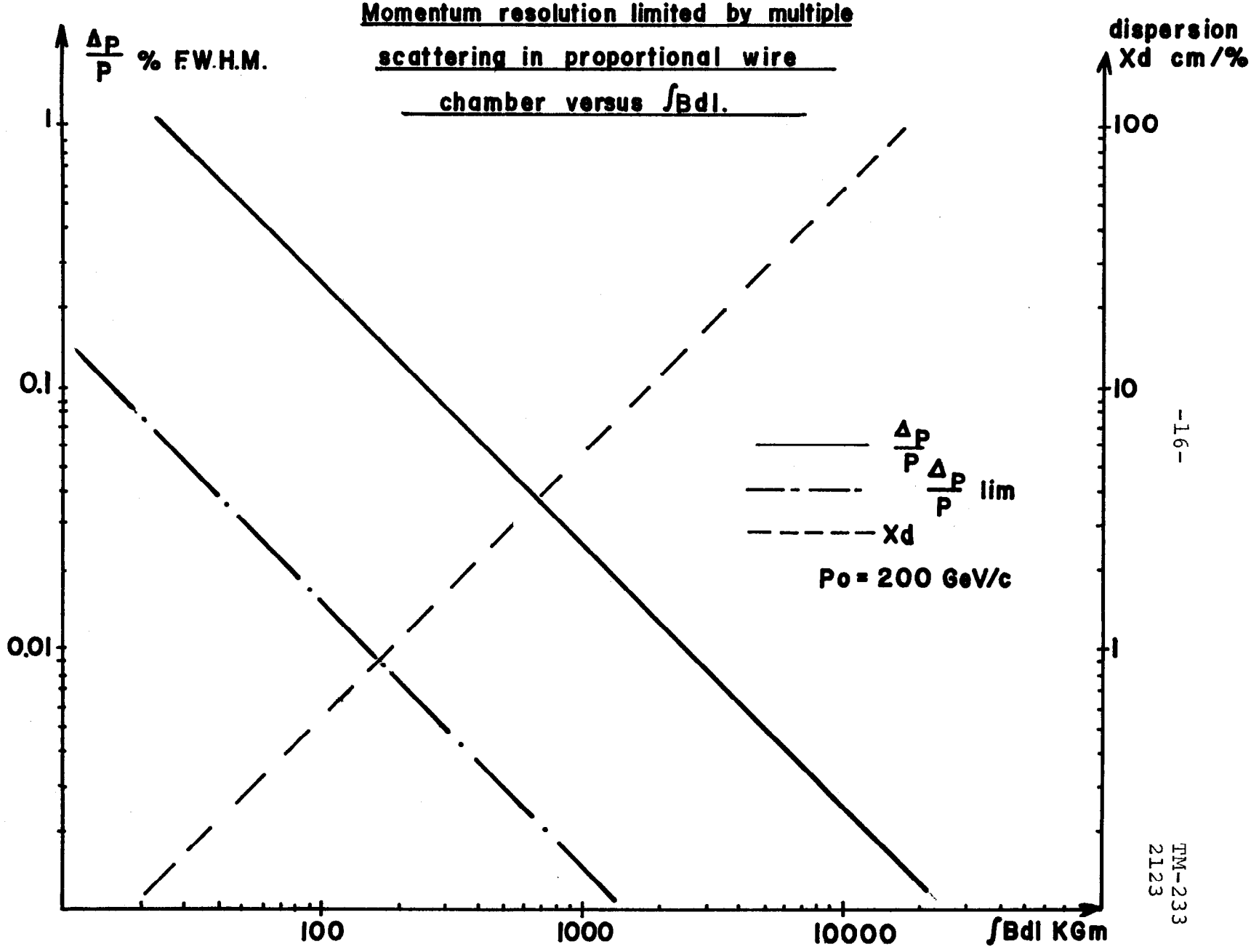

FIG. 8

TM-233
2123

IV. DISC Ĉerenkov COUNTER

In order to separate particles like, for example, pions from kaons at very high energies, it is sometimes necessary to introduce DISC Ĉerenkov counters into a focusing spectrometer or even into a certain section of a secondary particle beam. The design requirements for a DISC counter for high energy particles have been studied by R. Rubinstein.[3] In this report we pick up his conclusions and try to incorporate them in our spectrometer design criteria. The conclusions we will come to, apply also to secondary beam designs, where DISC counters are necessary.

To assure an adequate DISC counter performance with high efficiency and appropriate resolution, all particles passing through the counter must be parallel to its axis within $\pm\frac{\delta\theta'}{2}$. The angular aperture of the light acceptance diaphragm $\delta\theta'$ is related to the Ĉerenkov angle θ and the velocity resolution $\frac{\Delta\beta}{\beta}$ by

$$\tan\theta\delta\theta' = \frac{\Delta\beta}{\beta} = \frac{1}{2\gamma_K^2} - \frac{1}{2\gamma_\pi^2} \qquad (16)$$

Since it is technically difficult to make $\delta\theta'$ smaller than 0.1 mrad, we take $\delta\theta' = 0.1$ mrad, and calculate $\frac{\Delta\beta}{\beta}$ for 200 GeV/c pions and kaons.

$$\frac{\Delta\beta}{\beta} = 2.8\ 10^{-6} \qquad (17)$$

with $2\gamma_K^2 = 32.8\ 10^4$

and $2\gamma_\pi^2 = 4.1\ 10^6 \qquad (18)$

From equation (16) we than obtain a Čerenkov angle

$$\tan \theta \approx \theta \approx 28 \text{ mrad}$$

This angle is important for determining the necessary length L' of the Čerenkov counter. According to Ref. 3, L' can be 4m or smaller to assure a reasonable efficiency of the counter.

The following points require special attention in beam and spectrometer designs in connection with DISC Čerenkov counters:

1. In any point-to-parallel focusing system off axis particles at the focus will not go parallel through the DISC counter if the counter axis coincides with the optical axis of the system.
2. Particles with momenta not equal to the central momentum of the system will deviate from parallelism due to chromatic aberrations in the focusing system.

For a better understanding how large these effects can be, we made a quantitative study with a point-to-parallel doublet. We assumed 6m long quadrupole magnets with a bore 2R = 10cm, a maximum field gradient ∇B = 2kG/cm, a distance D = 30cm and an object length O = 12m. We only considered the extreme rays (not the beam envelope!) with $\theta_H = \pm 1.33$ mrad and $\theta_V = \pm 3.75$ mrad and calculated $\delta\theta'_H$ and $\delta\theta'_V$ in first and

second order from

$$\delta\theta_H' = R_{21}x_o + T_{216}x_o \frac{\delta p}{p} + T_{226}\,\theta_H \frac{\delta p}{p}$$

$$\delta\theta_V' = R_{43}y_o + T_{436}y_o \frac{\delta p}{p} + T_{446}\,\theta_V \frac{\delta p}{p} \qquad (19)$$

for different momentum spreads $\frac{\delta p}{p}$ as a function of the beam spot-size x_o and y_o at the focus. The first and second order matrix elements R_{ij} and T_{ijk} we obtained from a second order "Transport" run on an IBM-360 computer. The results are plotted in Fig. 9. It has to be pointed out that these results are somewhat pessimistic, since we have considered only the extreme rays. A beam profile calculation with a Monte Carlo program and a higher order ray tracing program will clearly give more realistic results. These calculations are under way.

If we assume small beam spot-sizes, equation (19) reduces to

$$\delta\theta_H' \approx T_{226}\,\theta_H \frac{\delta p}{p} \qquad (20)$$

and

$$\delta\theta_V' \approx T_{446}\,\theta_V \frac{\delta p}{p}$$

Since $T_{226} \approx T_{446}$ = const. for $R \ll L$, we are able to scale the results in Fig. 9 for different horizontal and vertical acceptances θ_H and θ_V by the relation

$$\frac{\delta\theta_H'}{\delta\theta_V'} \approx \frac{\theta_H}{\theta_V} \qquad (21)$$

When we keep in mind, that for the proper separation of pions

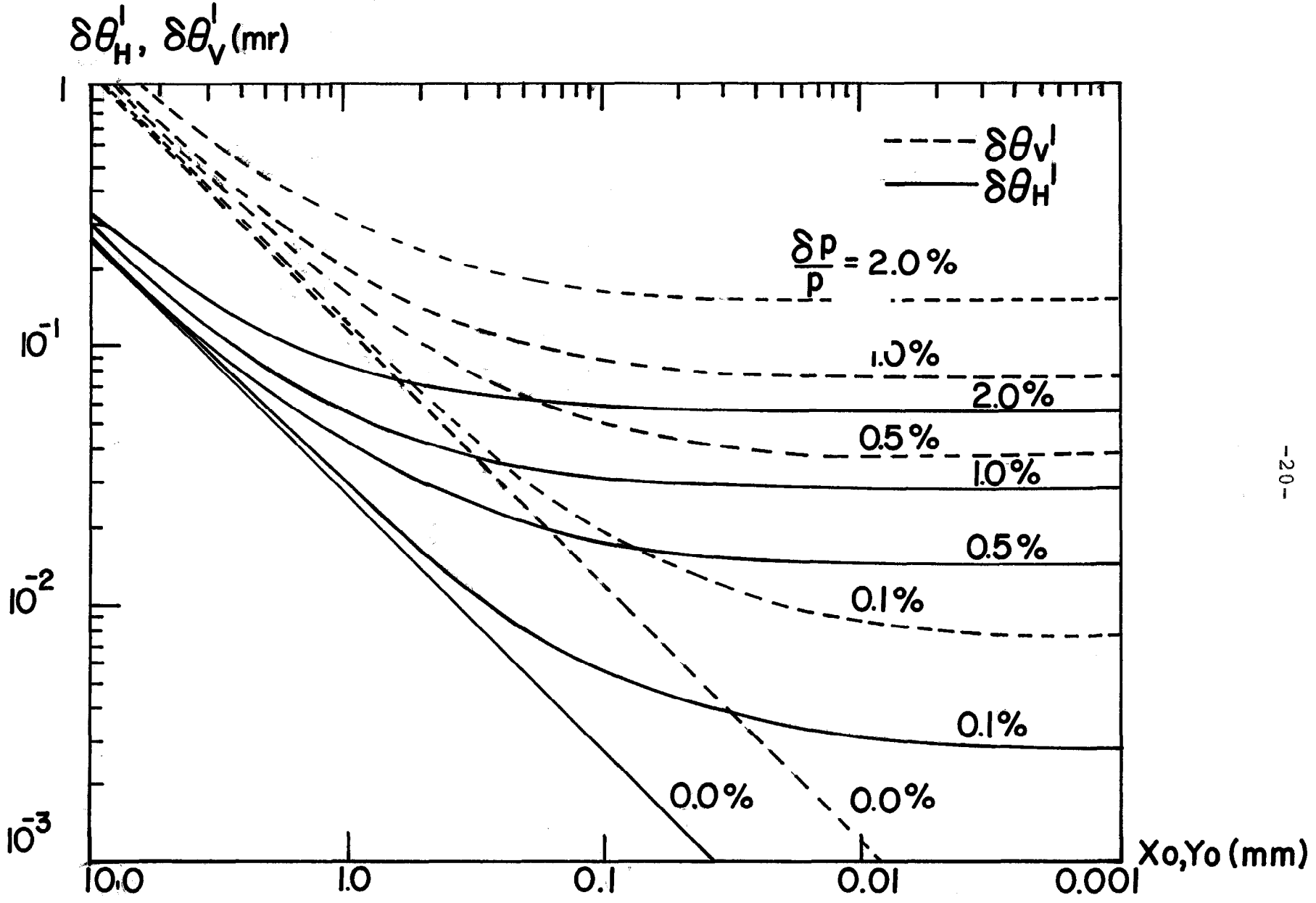
$\delta\theta_H'$, $\delta\theta_V'$ (mr)
1
10^{-1}
10^{-2}
10^{-3}
$\delta\theta_V'$
$\delta\theta_H'$
$\frac{\delta p}{p}$ = 2.0%
1.0%
2.0%
0.5%
1.0%
0.5%
0.1%
0.1%
0.0%
0.0%
10.0
1.0
0.1
0.01
0.001
Xo,Yo (mm)

Fig. 9

and kaons at 200 GeV/c, a DISC Čerenkov counter tolerates $\delta\theta' = \pm$ 0.05 mrad, with its present technique, we come to the following conclusions:

1. A DISC counter can be made to work in a high energy beam or spectrometer, if the beam spot-size at the focus is on the order of ±1mm or smaller, and the horizontal and vertical beam divergence is not much larger than ±1 mrad.
2. A beam momentum spread of ±1% is acceptable. This can easily be achieved by closing the momentum slit in a high energy beam. In the case of a focusing spectrometer, a momentum pre-selection can be done by either using the DISC counter as a tagging counter, where it will be triggered by particles after their momentum selection in the spectrometer, or by introducing a small trigger counter at the momentum focus. It is worth mentioning, that a change in β due to the momentum spread $\frac{\delta p}{p} \approx 1\%$ for 200 GeV/c kaons, is $\frac{\delta\beta}{\beta} = 0.06\ 10^{-6}$, which is considerably smaller than the resolution $\frac{\Delta\beta}{\beta} = 2.8\ 10^{-6}$ required for separating kaons from pions.

IV. FOCUSING SPECTROMETER VERSUS NON-FOCUSING SPECTROMETER

It is difficult to make a valid comparison between a focusing and a non-focusing spectrometer, since their applications are generally different. If we still want to do so in a quantitative way, we have to choose a model which is somewhat realistic and applicable to a large number of experiments, which can be done with either of those spectrometers at very high energies. For our comparison we have chosen a focusing spectrometer of the type we have described earlier in this report (Fig. 7), and a non-focusing spectrometer of the simplest type shown in Fig. 10.

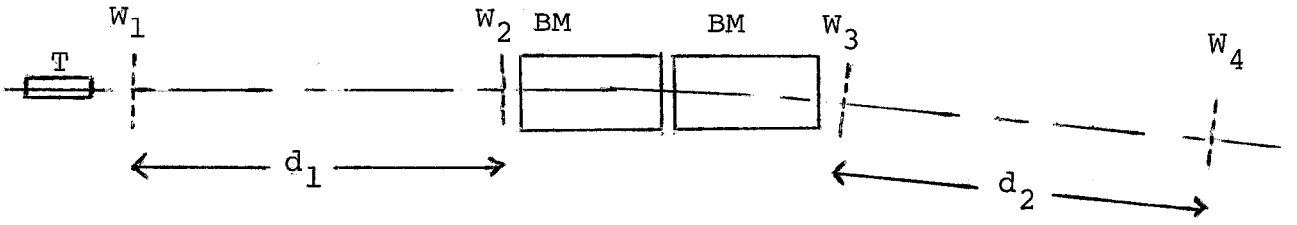

Fig. 10

In both cases we introduced wire proportional chambers W_1, W_2... as detectors, since they have a small deadtime and a good spatial resolution. We take p = 200 GeV/c, $\frac{\Delta p}{p} = \pm 0.05\%$ and $\Delta\Omega = 16\mu$ steradian as fixed parameters for both types of spectrometers and calculate within our model a list of parameters which we want to compare for both cases (Table I). From Figs. 4 and 6, and from the results of the previous paragraphs, we obtain the essential parameters for our focusing

spectrometer. In the case of the non-focusing spectrometer the momentum resolution is given by

$$\frac{\Delta p}{p} = \frac{\Delta \alpha}{\alpha} \tag{22}$$

where $\alpha = \frac{0.03 \int B d\ell}{p}$ is the bending angle in radians and $\Delta\alpha$ is the accuracy of the angle measurement with the chambers W_1, W_2, W_3, and W_4. If we addume $d = d_1 = d_2$ we obtain

$$\Delta \alpha = \frac{2\ \Delta x}{d} \tag{23}$$

with Δx the spatial resolution in the proportional chambers. With (23) we rewrite equation (22)

$$\int B d\ell \quad d = \frac{2\ \Delta x\ 200}{0.03\ \frac{\Delta p}{p}} \tag{24}$$

That means for a given $\frac{\Delta p}{p} = \pm\ 0.05\%$ and a given $\Delta x = \pm\ 0.5$mm the product

$$\int B d\ell\ d\ = 1.33\ 10^4\ \ \text{kG m}^2 \tag{25}$$

is a constant. In the case of a non-focusing spectrometer, d has to be about 50m in order to keep $\int B d\ell$ = 265 kGm, as it is required for the same momentum resolution in the case of a focusing spectrometer. This makes a non-focusing system nearly two times longer than a focusing system, which has with 4 quadrupoles = 24m, 3 bending magnets (B_{max} = 15kG) = 18m, and an object and image distance = 24m, a total length of about 70 meters. By taking multiple scattering in air outside the bending magnets into account, it is interesting to note that with d = 11m, the multiple scattering angle $\Delta\alpha'$ in air already

exceeds $\Delta\alpha = \pm 2.0\ 10^{-5}$ [rad], which was necessary to yield $\frac{\Delta p}{p} = \pm 0.05\%$ for a given $\int Bd\ell = 265$ kGm. Multiple scattering in air can usually be reduced to a minimum by introducing vacuum pipes or helium bags in the system. This is generally true for both the focusing and non-focusing system.

The multiple scattering angle $\Delta\alpha_2'$ in the proportional wire chambers W_2, W_3 is with $\Delta\alpha_2' = \pm 4.8\ 10^{-6}$ [radian] relatively small compared to $\Delta\alpha$. In order to make the length of the two spectrometers compatible, the $\int Bd\ell$ in the case of a non-focusing spectrometer has to be at least two times larger than in the case of a focusing system.

The solid angle acceptance for a non-focusing spectrometer is usually determined by the width W, the gap g and the length of the bending magnets. In our calculations we have assumed a horizontal angular acceptance $2\theta_H = 7.5$ mrad, which corresponds to the maximum vertical angular acceptance of our focusing spectrometer. For $\Delta\Omega = 16\mu\text{ster} = \pi\theta_H\ \theta_V$ we obtain $\theta_V = 1.36$ mrad or a width to gap ratio of approximately 3:1. By calculating the magnet width W for the different spectrometers, listed in Table I, we have taken into account the bending angles and non-wedge shaped bending magnets with the maximum length L = 6m and a maximum field B = 15kG.

Our magnet cost estimates are based on:

Quadrupole:

L = 6m B_{max} = 10kG 2R = 10cm $45,000 each

Magnet:

L = 6m B_{max} = 15kG W = 25cm g = 7.5cm \$100,000 each

L = 6m B_{max} = 15kG W = 60cm g = 20cm \$250,000 each

The cost estimate is correct within 30% and scales with the length of the magnet.

If we summarize the results we obtained from this comparison, we come to the following conclusions:

1. A focusing spectrometer is less costly than a non-focusing spectrometer. This cost difference reflects not only back in the magnet costs, but also in the number and the size of the detectors as well as their electronical data handling. The size of the detectors in the non-focusing case is considerably larger.
2. DISC Čerenkov counters cannot be used in non-focusing spectrometers.
3. Specially designed magnets are not necessarily required for a focusing spectrometer, since existing secondary beam elements are usually adequate.
4. In both cases a field homogeneity of 5×10^{-4} for $\int Bd\ell$ is required for the various orbits through the bending magnets if the resolution is to be maintained without making corrections. Inhomogeneities of a few times this value can be tolerated since relatively simple corrections can then be made to achieve the required precision. Large inhomogeneities

TABLE I.

Comparison Focusing Spectrometer Versus Nonfocusing Spectrometer

Constant in both cases:

$p = 200$ GeV/c $\quad \frac{\Delta p}{p} = \pm 0.05\% \quad \Delta\Omega = 16$ μster.

	Focusing Spectrometer	Nonfocusing Spectrometer
Total length	70 m	120 m
Detector	Wire proportional chamber	Wire proportional chamber
Number of detector	3	4
Spatial resolution in detectors	±0.5 mm	±0.5 mm
Distance between detectors before or behind spectrometer magnets	12 m	50 m
$\frac{\Delta p}{p}$ limited by multiple scattering in detectors	±0.004%	±0.012%
Number of quadrupoles	4	0
Number of bending magnets (B_{max}=15kG, length 6m each)	3	3
Magnet gap g	7.5 cm	20 cm
Magnet width W	25 cm	60 cm
DISC counters	yes	no
Magnet cost estimate includes quadrupoles	$480,000	$750,000

must be avoided since magnet tracking will in most cases require large amounts of computer time.

On the basis of physics, engineering and economics, a focusing spectrometer is superior to a non-focusing spectrometer for momentum measurements with high resolutions in the multi-GeV region.

APPENDIX

Method for Calculating Multiple Scattering Effects in Focusing System

It has been shown by Fermi[4], that the angular distribution of multiple scattered particles is Gaussian at every thickness of absorber and irrespective of position in the absorber. The rms projected angles can be calculated from the well known formula

$$\alpha = \frac{15\ [\text{MeV}]}{\text{pv}\ [\text{MeV}]}\sqrt{\frac{L}{L_{rad}}}\ (1 + \varepsilon) \qquad (26)$$

with the particle trajectory length L in the absorber and with $\varepsilon < 1/10$ for $L > 1/10\ L_{rad}$. Similarly at every thickness the distribution in space of multiple scattered particles, irrespective of angle, is Gaussian. The rms projected lateral displacement δ of particles traversing an absorber of thickness L is then

$$\delta = \frac{L\alpha}{\sqrt{3}} \qquad (27)$$

If we assume a zero energy loss of the particles in the absorber, we can easily calculate the multiple scattering effects

of various absorbers in our focusing system to any point further downstream. Since the spatial distributions and angular distributions are Gaussian and independent of what happened to the particles before they were multiply scattered, we can combine the projected angles as well as the lateral displacements at various points in the system by adding them in quadrature after we have multiplied them with the appropriate transfer matrices.

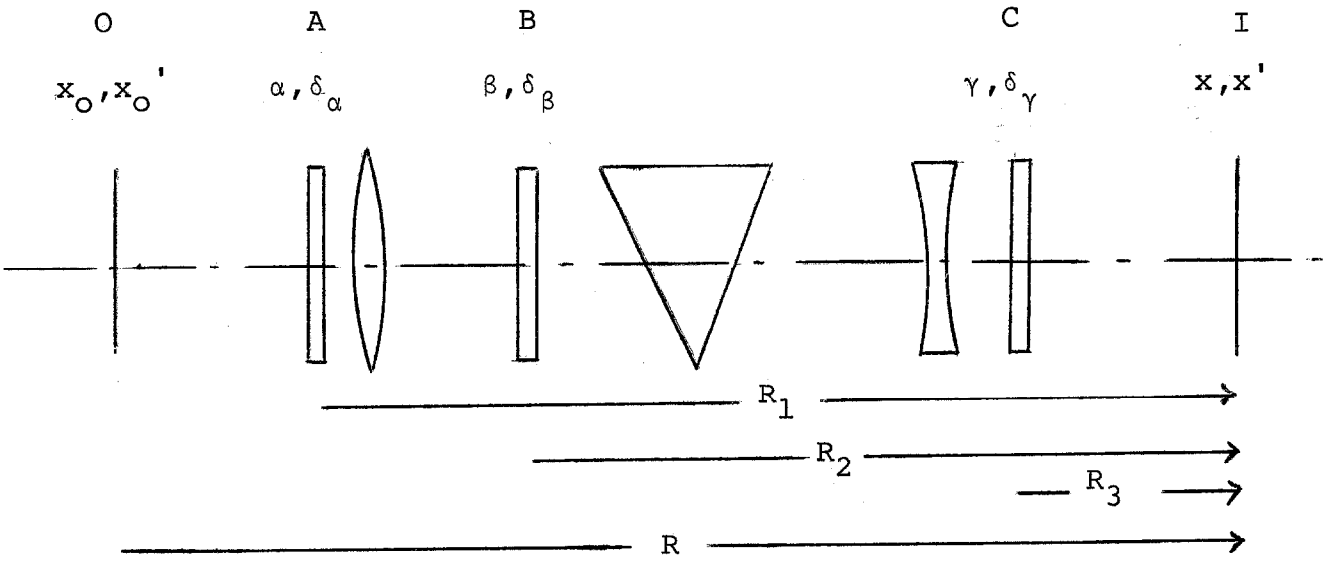

Fig. 11

As an example, we show in Fig. 11 a focusing system with three absorbers, A, B, and C. We assume that particles enter our focusing system at a plane 0 (object plane) with a constant momentum, a horizontal displacement x_o and an angle x_o'. If we know the transfer matrix R we can calculate their

angle x' and their displacement x at a plane I (image plane) from

$$\begin{pmatrix} x \\ x' \\ \vdots \end{pmatrix} = R \begin{pmatrix} x_o \\ x'_o \\ \vdots \end{pmatrix} \tag{28}$$

Particles which undergo multiple scattering in the absorbers A B and C will have angular and displacement uncertainties x'_α, x'_β, x'_γ and x_α, x_β, x_γ in plane I, which we obtain by multiplying the multiple scattering angles α, β, γ, and the displacements δ_α, δ_β, δ_γ with the appropriate transfer matrices R_1, R_2, R_3:

$$\begin{aligned} \begin{pmatrix} x_\alpha \\ x'_\alpha \end{pmatrix} &= R_1 \begin{pmatrix} \delta_\alpha \\ \alpha \end{pmatrix} \\ \begin{pmatrix} x_\beta \\ x'_\beta \end{pmatrix} &= R_2 \begin{pmatrix} \delta_\beta \\ \beta \end{pmatrix} \\ \begin{pmatrix} x_\gamma \\ x'_\gamma \end{pmatrix} &= R_3 \begin{pmatrix} \delta_\gamma \\ \gamma \end{pmatrix} \end{aligned} \tag{29}$$

The combined uncertainties

$$\begin{pmatrix} x_{ms} \\ x_{ms'} \end{pmatrix} = \begin{pmatrix} \sqrt{x_\alpha^2 + x_\beta^2 + x_\gamma^2} \\ \sqrt{x_\alpha'^2 + x_\beta'^2 + x_\gamma'^2} \end{pmatrix} \tag{30}$$

give us the smear of the angle and displacement of the particles in the image plane

$$\begin{pmatrix} x \pm x_{ms} \\ x' \pm x_{ms}' \end{pmatrix} \tag{31}$$

The displacements δ_α, δ_β, δ_γ are in practice very small, because one normally avoids to have heavy and thick material in a focusing system. From Eq. (8) we then conclude that the smear of the displacement in the image plane due to multiple scattering is proportional to the R_{12} and respectively R_{34} matrix elements of the appropriate transfer matrix, or in other words, to the amplitude of the sine-like function at the place, where the multiple scattering occurs (for notation see Ref. 1). Therefore, if one has the choice, necessary detectors or any material should be placed in the focusing system, where the sine-like function is small.

REFERENCES

[1] K. L. Brown, SLAC Report No. 75.

[2] K. L. Brown, B. K. Kear, S. K. Howry, SLAC Report No. 91.

[3] R. Rubinstein, TM-203, 2526.

[4] B. Rossi, K. Greisen, Rev. Mod. Phys. 13, 240 (1941).